

Benchmark of quantum-inspired heuristic solvers for quadratic unconstrained binary optimization

Hiroki Oshiyama¹ and Masayuki Ohzeki¹

¹ Graduate School of Information Sciences, Tohoku University, Sendai 980-8579, Japan

ABSTRACT

Recently, inspired by quantum annealing, many solvers specialized for unconstrained binary quadratic programming problems have been developed. For further improvement and application of these solvers, it is important to clarify the differences in their performance for various types of problems. In this study, the performance of four quadratic unconstrained binary optimization problem solvers, namely D-Wave Hybrid Solver Service (HSS), Toshiba Simulated Bifurcation Machine (SBM), Fujitsu Digital Annealer (DA), and simulated annealing on a personal computer, was benchmarked. The problems used for benchmarking were instances of real problems in MQLib, instances of the SAT-UNSAT phase transition point of random not-all-equal 3-SAT (NAE 3-SAT), and the Ising spin glass Sherrington-Kirkpatrick (SK) model. Concerning MQLib instances, the HSS performance ranked first; for NAE 3-SAT, DA performance ranked first; and regarding the SK model, SBM performance ranked first. These results may help understand the strengths and weaknesses of these solvers.

1 Introduction

Quantum annealing (QA)^{1,2}, which is a quantum algorithm for solving combinatorial optimization problems, has attracted a great deal of attention because it is implemented using real quantum systems by D-Wave Systems Inc.^{3,4}, aiming at becoming more powerful than classical algorithms such as simulated annealing (SA)^{5,6}. To use the current D-Wave's QA device, a combinatorial optimization problem must be mapped to a quadratic unconstrained binary optimization (QUBO) problem. QUBO is an optimization problem of binary variables $x_i \in \{0, 1\}$, where $i \in \{1, 2, \dots, N\}$, and its cost function to be minimized is defined as

$$E(\mathbf{x}) = \sum_{i,j} Q_{i,j} x_i x_j, \quad (1)$$

where $Q_{i,j}$ is a real number called QUBO matrix element. In general, QUBO is NP-hard⁷, and many NP-complete problems and combinatorial optimization problems are mapped to QUBO⁸.

Although current QA devices have limited capability owing to hardware implementation limitations, in anticipation of future developments of QA devices, methods using QUBO models for solving real-world problems in a variety of fields have been actively studied^{9–15}. Inspired by this trend, several sophisticated heuristic QUBO solvers have been developed and commercialized^{16–19}. It is highly non-trivial to determine whether a particular algorithm is more powerful than another because the performance of heuristic algorithms varies depending on the target problem. For successful application to real-world problems and further development of these QUBO solvers, it is necessary to clarify the strengths and weaknesses of each solver for various types of QUBO problems. In this study, we benchmarked the performance of three commercialized QUBO solvers including one using a real QA device: D-Wave Hybrid Solver Service (HSS), Toshiba Simulated Bifurcation Machine (SBM), and Fujitsu Digital Annealer (DA); three types of problem sets were used.

The remainder of this paper is organized as follows. In Sec. 2, we briefly explain the solvers benchmarked. In Sec. 3, the definition of the problem instances used for benchmarking are provided. In Sec. 4, we present the results of the benchmarking experiment. Finally, in Sec. 5, we summarize our results and conclusions.

2 QUBO solvers

In this section, we briefly explain the four solvers used in this study. Three commercial solvers were benchmarked. For comparison, we also experimented with SA on a personal computer.

The first solver is HSS, commercialized by D-Wave Systems Inc.¹⁶. This solver is a so-called quantum-classical hybrid algorithm that employs QA as an accelerator. Note that the actual implementation of the algorithm is not open to the public. Thus, it is unclear how QA is used internally. We used HSS hybrid BQM solver, version 2.0, which can manage up to one million variables and two hundred million couplings²⁰.

The second solver is SBM, commercialized by Toshiba¹⁸. This solver, inspired by QA, uses the adiabatic time evolution of Kerr-nonlinear parametric oscillators (KPOs)²¹. The dynamics in the classical limit of KPOs can be quickly computed in classical computers by solving the independent equations of motion in parallel¹⁸. We use SBM PoC version 1.2, which can manage all-to-all coupling of up to 10000 variables²². In this study, we used the `autoising` solver; the calculation parameters of SBM were not specified.

The third solver is DA, commercialized by Fujitsu¹⁹. DA uses an SA-specific hardware architecture to accelerate SA calculation^{23,24}. Although DA does not use quantum algorithms, it is inspired by D-Wave devices in the sense that the hardware is specialized for QUBO solving. We used `fujitsuDA2PT` solver, which can manage all-to-all coupling of up to 8192 variables.

For comparison with these commercial solvers, we ran SA using the open-source software D-Wave `neal`, version 0.5.7²⁵, on a personal computer. The CPU used in the experiment was Intel(R) Core(TM) i9-9900K, and single-threaded runs were performed.

3 Problem instances for benchmarking

In this section, we explain the three problem sets used in the conducted benchmarking.

3.1 MQLib repository instances

We used the same set of 45 problems used in the benchmarks presented in HHS's white paper^{16,26}. This problem set is extracted from the MQLib repository, and some of the problems have their origin in real-world problems, such as image segmentation²⁷. This problem set was reported to be time-consuming to solve because of all the heuristics contained in the MQLib library. Concerning benchmarking, a 20-minute run is recommended for each problem¹⁶. The 45 problems are uniformly classified into nine classes: three classes according to size (small: $1000 \leq N \leq 2500$, medium: $2500 < N \leq 5000$, and large: $5000 < N \leq 10000$) and three classes according to edge density (sparse: $d \leq 0.1$, medium: $0.1 < d \leq 0.5$, and dense: $0.5 < d$), where d is the number of edges divided by the number of edges in a complete graph of the same size¹⁶.

3.2 Not-All-Equal 3-SAT

Not-all-equal 3-SAT (NAE 3-SAT) is a variant of the Boolean satisfiability problem and is an NP-complete problem²⁸. NAE 3-SAT requires at least one literal to be true and at least one literal to be false in each clause with three literals. The cost function of a random NAE 3-SAT with N variables and M clauses is expressed in a straightforward manner in the Ising model with $\sigma_i \in \{-1, 1\}$, where $1 \leq i \leq N$:

$$E(\boldsymbol{\sigma}) = \frac{1}{4} \sum_{m=1}^M (\zeta_{m,1} \zeta_{m,2} \sigma_{i_{m,1}} \sigma_{i_{m,2}} + \zeta_{m,2} \zeta_{m,3} \sigma_{i_{m,2}} \sigma_{i_{m,3}} + \zeta_{m,3} \zeta_{m,1} \sigma_{i_{m,3}} \sigma_{i_{m,1}} + 1), \quad (2)$$

where $i_{m,l} \in \{1, 2, \dots, N\}$ and $\zeta_{m,l} \in \{-1, 1\}$ for $1 \leq m \leq M$ and $1 \leq l \leq 3$ are random variables that follow a discrete uniform distribution; $\zeta_{m,l} = -1$ corresponds to the negation of the l -th Boolean variable in clause m . Each clause has three different variables, i.e., $i_{m,l} \neq i_{m,l'}$ if $l \neq l'$. If the minimum of $E(\boldsymbol{\sigma})$ in Eq. (2) is 0 for a given formula, it is satisfiable (SAT); otherwise, it is unsatisfiable (UNSAT). The QUBO formulation as in Eq. (1) can be easily obtained from this Ising formulation by the variable transformation $x_i = (\sigma_i + 1)/2$.

When the clause-to-variable ratio is $M/N = 2.11$, the SAT-UNSAT phase transition occurs, and problem instances are most difficult to solve^{29,30}. In this study, we used randomly generated instances with this critical clause-to-variable ratio for benchmarking.

3.3 Sherrington-Kirkpatrick model

The Sherrington-Kirkpatrick (SK) model is an Ising spin glass model with infinite spatial dimensions^{31,32}. The cost function of N variables with no external field is expressed as

$$E(\boldsymbol{\sigma}) = \frac{1}{\sqrt{N}} \sum_{1 \leq i < j \leq N} J_{i,j} \sigma_i \sigma_j, \quad (3)$$

where $J_{i,j}$ is a random Gaussian variable. As previously explained, the QUBO formulation can be easily obtained. The mean field analysis shows that the energy landscape of the SK model has a many-valley structure separated by asymptotically infinitely large energy barriers, which implies that it is extremely difficult to find the exact solution³³. In this study, we used randomly generated instances with $J_{i,j}$ presenting zero mean and unity standard deviation for benchmarking.

	Small				Medium				Large				Total			
	HSS	SBM	DA	SA	HSS	SBM	DA	SA	HSS	SBM	DA	SA	HSS	SBM	DA	SA
Sparse	5	4	2	1	1	0	2	2	2	2	1	0	8	6	5	3
Medium	5	3	1	1	1	1	2	1	1	1	5	0	7	5	8	2
Dense	4	3	1	0	3	2	2	1	0	0	4	1	7	5	7	2
Total	14	10	4	2	5	3	6	4	3	3	10	1	22	16	20	7

Table 1. Number of wins for a 5-min experiment of MQLib instances. The row direction is classified in terms of size (Small, Medium, and Large), whereas the column direction is classified in terms of edge density (Sparse, Medium, and Dense).

4 Results

In this section, we present benchmarking results for each of the three problem sets introduced in the previous section. In the results shown below, the network time required to send the instance and receive the result was ignored in the measurement of execution time. Regarding HSS, the number of seconds specified in `time_limit` was used as the execution time. For SBM, the time specified in `timeout` was used as the execution time. Concerning DA, there was no parameter to specify the execution time directly, so `total_elapsed_time` recorded in the response file was used as the execution time. Finally, for SA with D-Wave neal, we measured the time taken for the `sample` function to finish.

4.1 MQLib instances

First, we present the results for a 5-min experiment of the instances from the MQLib repository. For HSS and SBM, the execution time was set to 5 min. For DA, `number_replicas` was set to 128 and `number_iterations` was adjusted for each instance so that the deviation of execution time in 5 min was within 20 s. Concerning SA, `num_sweeps` was adjusted for each instance such that the execution time was 5 min. Table 1 shows the number of wins for each solver; this number was counted when the solver obtained the best solution. If there was more than one solver with the best solution, the number of wins was counted for all of them. The total result for all classes was that HSS won most of the problems (22), followed by DA (20), SBM (16), and SA (7). The results for each class classified by size show that HSS won the most for the small class, while DA won the most for the medium and large classes. The results for each class classified by edge density show that, for Sparse class, HSS won the most, for Medium class, DA won the most, and HSS and DA won the most. The number of wins of SA was only 2 at most, and most of the time, it was 0 or 1 for each of the nine classes. Tables 2-10 show the value of the cost function obtained by each solver for each instance; this value is the ratio of the best value found in this experiment. For almost all instances, the solutions by HSS and SBM were in agreement by more than three orders of magnitude with the best solution found in this experiment. The solutions by DA tended to have larger differences from the best solution compared to other solvers. The lowest values of the cost function found in this benchmarking are listed in Table 11.

input	size	density	HSS	SBM	DA	SA
g000989	2319	0.00086	1.0	1.0	1.0	0.998708
g003215	2206	0.00093	1.0	0.999457	0.998103	0.997985
g001269	2294	0.0017	1.0	1.0	1.0	0.999847
g000421	2034	0.0038	1.0	1.0	0.985010	0.999303
g002440	2242	0.044	1.0	1.0	0.999213	1.0

Table 2. Values of cost functions, ratio to the best solution found in a 5-min experiment of MQLib instances for Small and Sparse classes. The first row shows the instance name, the second row presents the number of variables, the third row contains the edge density, and the fourth and subsequent rows show the results for each solver. The values are computed in single precision from the obtained solution of binary variables; they are shown with six decimal places. The best solutions obtained in this benchmarking are shown in bold.

input	size	density	HSS	SBM	DA	SA
g000432	2153	0.11	1.0	0.999958	0.999045	0.999974
g000524	2218	0.14	1.0	1.0	1.0	1.0
g002586	2079	0.16	1.0	1.0	0.999102	0.999890
g001327	2318	0.3	1.0	1.0	0.999300	0.999928
g001469	2412	0.46	1.0	0.999824	0.998105	0.999911

Table 3. Results for Small and Medium classes, same as Table 2.

input	size	density	HSS	SBM	DA	SA
g002600	2432	0.85	1.0	0.999999	0.999505	0.999976
g000969	2453	0.86	1.0	1.0	0.995138	0.999645
g002898	2041	0.86	1.0	1.0	1.0	0.999996
g001581	2383	0.86	0.999999	1.0	0.999640	1.000000
g000788	2342	0.88	1.0	0.999860	0.999492	0.999959

Table 4. Results for Small and Dense classes, same as Table 2.

input	size	density	HSS	SBM	DA	SA
g000377	3398	0.00069	0.998763	0.999890	1.0	0.998353
g002569	2815	0.0011	1.0	0.999459	0.983877	0.998564
g001086	3706	0.0016	0.998913	0.998673	0.985686	1.0
g001337	2850	0.051	0.999975	0.999923	1.0	0.999931
g000283	3364	0.072	0.999946	0.999905	0.997073	1.0

Table 5. Results for Medium and Sparse classes, same as Table 2.

input	size	density	HSS	SBM	DA	SA
g002512	4731	0.12	0.999913	0.999861	1.0	0.999980
g000802	3956	0.13	0.999990	1.0	0.998449	0.999919
g003059	3447	0.14	0.999973	0.999939	1.0	0.999962
g002332	3181	0.22	0.999994	0.999996	0.999156	1.0
g002034	2528	0.35	1.0	0.999997	0.999201	0.999979

Table 6. Results for Medium and Medium classes, same as Table 2.

input	size	density	HSS	SBM	DA	SA
g003198	3972	0.74	1.0	0.999956	0.999616	0.999979
g002207	2677	0.74	1.0	1.0	1.0	0.999954
g001913	3865	0.75	1.0	0.999786	0.999333	0.999643
g001393	3938	0.83	0.999967	1.0	1.0	0.999886
g002370	3884	0.84	0.999716	0.999843	0.997744	1.0

Table 7. Results for Medium and Dense classes, same as Table 2

input	size	density	HSS	SBM	DA	SA
imgseg-216041	7724	0.00039	1.0	0.999919	0.996163	0.995890
imgseg-376020	7455	0.00049	1.0	0.999522	0.989190	0.998811
g001883	6831	0.00059	1.000000	1.0	0.999489	0.999998
g000644	10000	0.0016	0.999307	1.0		0.999752
g000476	8000	0.002	0.999457	0.999766	1.0	0.999860

Table 8. Results for Large and Sparse classes, same as Table 2. For input g001883, HSS and SBM had almost the same value of the cost function, while the solution configurations were truly different from each other. The result of DA for input g000644 is blank because DA can only manage 8192 variables.

input	size	density	HSS	SBM	DA	SA
g002312	6395	0.19	0.999957	0.999054	1.0	0.999930
g002563	6279	0.19	0.999842	0.999966	1.0	0.999945
g000495	5438	0.21	0.999941	0.999980	1.0	0.999958
g002204	5368	0.44	1.0	1.0	1.0	0.999903
g000503	5046	0.45	0.999954	0.999966	1.0	0.999983

Table 9. Results for Large and Medium classes, same as Table 2.

input	size	density	HSS	SBM	DA	SA
g002527	5378	0.59	0.999949	0.999574	1.0	0.999885
g001345	5066	0.74	0.999252	0.999004	0.475147	1.0
p7000-2	7001	0.8	0.999992	0.999748	1.0	0.999563
g002300	5038	0.94	0.999970	0.999988	1.0	0.999995
g001651	5819	0.97	0.999949	0.999913	1.0	0.999930

Table 10. Results for Large and Dense classes, same as Table 2.

4.2 NAE 3-SAT instances

Next, we present the results for the random NAE 3-SAT instances with a number of variables $N = 8192$ and a number of clauses $M = 17285$, i.e., instances with a clause-to-variable ratio $N/M \approx 2.11$. Figure 1 (a) shows the average of ten randomly generated instances of the cost function as a function of the execution time. As a reference, Fig. 1 (b) shows the results for ten different instances. Given that each data point was obtained from an independent run, a longer run may lead to a worse solution than a shorter run. In the range 100-600 s, DA presented the lowest value of the cost function, closely followed by SBM and SA; HSS presented the highest value. In the region below 100 s, SBM and SA showed lower energy than DA. Focusing on the slope in the region beyond 200 s, HSS was the steepest, while SBM and SA were almost flat. Therefore, it is likely that HSS can obtain a much better solution than SBM and SA in a longer calculation. DA presented a steeper slope than SBM and SA in the region that we could calculate. In summary, SBM and SA are better for short-time calculations, while DA and HSS are better for long-time calculations. The lowest values of the cost function in this experiment were obtained using DA.

4.3 SK model

Finally, we present the results for the SK model with 8192 variables. As with the NAE 3-SAT instances, the experiments were performed by varying the execution time. Figure 2 (a) shows the average of six randomly generated instances of the cost function as a function of the execution time. As a reference, Fig. 2 (b) shows the results for six different instances. SBM achieved the best solutions at the 100-s mark, with little energy change for longer runs. HSS and DA showed almost the same time dependence, although HSS provided a slightly better solution. In runs longer than 600 s, SA obtained as good solutions as HSS and DA, but due to the all-to-all coupling, its pre-processing calculation was expensive, requiring at least approximately 500 s for the total calculation time. In summary, SBM performs the best in terms of both computation time and solution quality. HSS and DA show similar performance.

5 Summary

In this study, we benchmarked the QUBO solvers, HSS, SBM, DA, and SA, using the instances from the MQLib repository, random NAE 3-SAT, and the SK model. HSS exhibited the steepest time dependence concerning the cost function on both NAE 3-SAT and SK models in the long-execution-time region, which implies that HSS can obtain good solutions in long runs. SBM showed the best performance on the SK model, while other solvers provided worse solutions than those given by SBM in a 100-s run, and even in runs longer than 600 s, while for the NAE-3AT problem, SBM showed almost the same time dependence regarding the cost function as SA. DA performed the best for the large-size MQLib instances and the NAE 3-SAT instances in the long-execution-time region. Interestingly, SBM and DA behaved almost identically for the NAE 3-SAT problem, whereas HSS and DA behaved almost identically for the SK model. It is an important challenge to understand the characteristics of each solver found in this study from the viewpoint of their algorithms.

Acknowledgements

We thank Murray Thom, Catherine McGeoch, and Hayato Goto for fruitful discussion on our benchmark tests. In addition, we acknowledge research supports on various aspects from D-Wave Systems Inc. and TOSHIBA CORPORATION. M. O. thanks financial support from the Next Generation High-Performance Computing Infrastructures and Applications R & D Program by MEXT, and MEXT-Quantum Leap Flagship Program Grant Number JPMXS0120352009.

References

1. Farhi, E. *et al.* A quantum adiabatic evolution algorithm applied to random instances of an np-complete problem. *Science* **292**, 472–475, DOI: [10.1126/science.1057726](https://doi.org/10.1126/science.1057726) (2001). <https://science.sciencemag.org/content/292/5516/472.full.pdf>.
2. Das, A. & Chakrabarti, B. K. Colloquium: Quantum annealing and analog quantum computation. *Rev. Mod. Phys.* **80**, 1061–1081, DOI: [10.1103/RevModPhys.80.1061](https://doi.org/10.1103/RevModPhys.80.1061) (2008).
3. Johnson, M. *et al.* Quantum annealing with manufactured spins. *Nature* **473**, 194–8, DOI: [10.1038/nature10012](https://doi.org/10.1038/nature10012) (2011).
4. Harris, R. *et al.* Experimental investigation of an eight-qubit unit cell in a superconducting optimization processor. *Phys. Rev. B* **82**, 024511, DOI: [10.1103/PhysRevB.82.024511](https://doi.org/10.1103/PhysRevB.82.024511) (2010).
5. Kirkpatrick, S., Gelatt, C. D. & Vecchi, M. P. Optimization by simulated annealing. *Science* **220**, 671–680, DOI: [10.1126/science.220.4598.671](https://doi.org/10.1126/science.220.4598.671) (1983). <https://science.sciencemag.org/content/220/4598/671.full.pdf>.
6. Fu, Y. & Anderson, P. W. Application of statistical mechanics to NP-complete problems in combinatorial optimisation. *J. Phys. A: Math. Gen.* **19**, 1605–1620, DOI: [10.1088/0305-4470/19/9/033](https://doi.org/10.1088/0305-4470/19/9/033) (1986).
7. Barahona, F. On the computational complexity of ising spin glass models. *J. Phys. A: Math. Gen.* **15**, 3241–3253, DOI: [10.1088/0305-4470/15/10/028](https://doi.org/10.1088/0305-4470/15/10/028) (1982).
8. Lucas, A. Ising formulations of many np problems. *Front. Phys.* **2**, 5, DOI: [10.3389/fphy.2014.00005](https://doi.org/10.3389/fphy.2014.00005) (2014).
9. Perdomo-Ortiz, A., Dickson, N., Drew-Brook, M., Rose, G. & Aspuru-Guzik, A. Finding low-energy conformations of lattice protein models by quantum annealing. *Sci. Reports* **2**, 571, DOI: [10.1038/srep00571](https://doi.org/10.1038/srep00571) (2012).
10. Garnerone, S., Zanardi, P. & Lidar, D. A. Adiabatic quantum algorithm for search engine ranking. *Phys. Rev. Lett.* **108**, 230506, DOI: [10.1103/PhysRevLett.108.230506](https://doi.org/10.1103/PhysRevLett.108.230506) (2012).
11. Babbush, R., Love, P. J. & Aspuru-Guzik, A. Adiabatic quantum simulation of quantum chemistry. *Sci. Reports* **4**, DOI: [10.1038/srep06603](https://doi.org/10.1038/srep06603) (2014).
12. Venturelli, D., Marchand, D. J. J. & Rojo, G. Quantum annealing implementation of job-shop scheduling (2016). [1506.08479](https://doi.org/10.1506.08479).
13. Mott, A., Job, J., Vlimant, J. R., Lidar, D. & Spiropulu, M. Solving a Higgs optimization problem with quantum annealing for machine learning. *Nature* **550**, 375–379, DOI: [10.1038/nature24047](https://doi.org/10.1038/nature24047) (2017).
14. Benedetti, M., Realpe-Gómez, J., Biswas, R. & Perdomo-Ortiz, A. Quantum-assisted learning of hardware-embedded probabilistic graphical models. *Phys. Rev. X* **7**, 041052, DOI: [10.1103/PhysRevX.7.041052](https://doi.org/10.1103/PhysRevX.7.041052) (2017).
15. Li, R. Y., Di Felice, R., Rohs, R. & Lidar, D. A. Quantum annealing versus classical machine learning applied to a simplified computational biology problem. *npj Quantum Inf.* **4**, 14, DOI: [10.1038/s41534-018-0060-8](https://doi.org/10.1038/s41534-018-0060-8) (2018).
16. D-wave hybrid solver service: An overview. https://www.dwavesys.com/sites/default/files/14-1039A-A_D-Wave_Hybrid_Solver_Service_An_Overview.pdf.

17. Inagaki, T. *et al.* A coherent ising machine for 2000-node optimization problems. *Science* **354**, 603–606, DOI: [10.1126/science.aah4243](https://doi.org/10.1126/science.aah4243) (2016). <https://science.sciencemag.org/content/354/6312/603.full.pdf>.
18. Goto, H., Tatsumura, K. & Dixon, A. R. Combinatorial optimization by simulating adiabatic bifurcations in nonlinear hamiltonian systems. *Sci. Adv.* **5**, DOI: [10.1126/sciadv.aav2372](https://doi.org/10.1126/sciadv.aav2372) (2019). <https://advances.sciencemag.org/content/5/4/eaav2372.full.pdf>.
19. Aramon, M. *et al.* Physics-inspired optimization for quadratic unconstrained problems using a digital annealer. *Front. Phys.* **7**, 48, DOI: [10.3389/fphy.2019.00048](https://doi.org/10.3389/fphy.2019.00048) (2019).
20. D-wave hybrid solver service + advantage: Technology update. https://www.dwavesys.com/sites/default/files/14-1048A-A_D-Wave_Hybrid_Solver_Service_plus_Advantage_Technology_Update.pdf.
21. Goto, H. Bifurcation-based adiabatic quantum computation with a nonlinear oscillator network: Toward quantum soft computing. *Sci. Reports* **6**, DOI: [10.1038/srep21686](https://doi.org/10.1038/srep21686) (2016).
22. Simulated bifurcation machine user manual. http://dfk66cqpwr4ko.cloudfront.net/user_manual_en_v1_20.pdf.
23. Matsubara, S. *et al.* Ising-model optimizer with parallel-trial bit-sieve engine. In Barolli, L. & Terzo, O. (eds.) *Complex, Intelligent, and Software Intensive Systems*, 432–438 (Springer International Publishing, Cham, 2018).
24. Tsukamoto, S., Takatsu, M., Matsubara, S. & Tamura, H. An accelerator architecture for combinatorial optimization problems. *Fujitsu Sci. Tech. J.* **53**, 8–13 (2017).
25. dwave-neal. <https://github.com/dwavesystems/dwave-neal>.
26. Hss overview whitepaper benchmarks. <https://github.com/dwavesystems/hss-overview-benchmarks>.
27. Dunning, I., Gupta, S. & Silberholz, J. What works best when? a systematic evaluation of heuristics for max-cut and QUBO. *INFORMS J. on Comput.* **30** (2018).
28. Darmann, A. & Döcker, J. On simplified np-complete variants of not-all-equal 3-sat and 3-sat (2019). [1908.04198](https://arxiv.org/abs/1908.04198).
29. Achlioptas, D., Chtcherba, A., Istrate, G. & Moore, C. The phase transition in 1-in-k sat and nae 3-sat. *Proc. Annu. ACM-SIAM Symp. on Discret. Algorithms* DOI: [10.1145/365411.365760](https://doi.org/10.1145/365411.365760) (2001).
30. Gent, I. P. & Walsh, T. The sat phase transition. In *ECAI* (1994).
31. Sherrington, D. & Kirkpatrick, S. Solvable model of a spin-glass. *Phys. Rev. Lett.* **35**, 1792–1796, DOI: [10.1103/PhysRevLett.35.1792](https://doi.org/10.1103/PhysRevLett.35.1792) (1975).
32. Mezard, M., Parisi, G. & Virasoro, M. *Spin Glass Theory And Beyond: An Introduction To The Replica Method And Its Applications*. World Scientific Lecture Notes In Physics (World Scientific Publishing Company, 1987).
33. Thouless, D. J., Anderson, P. W. & Palmer, R. G. Solution of 'solvable model of a spin glass'. *The Philos. Mag. A J. Theor. Exp. Appl. Phys.* **35**, 593–601, DOI: [10.1080/14786437708235992](https://doi.org/10.1080/14786437708235992) (1977). <https://doi.org/10.1080/14786437708235992>.

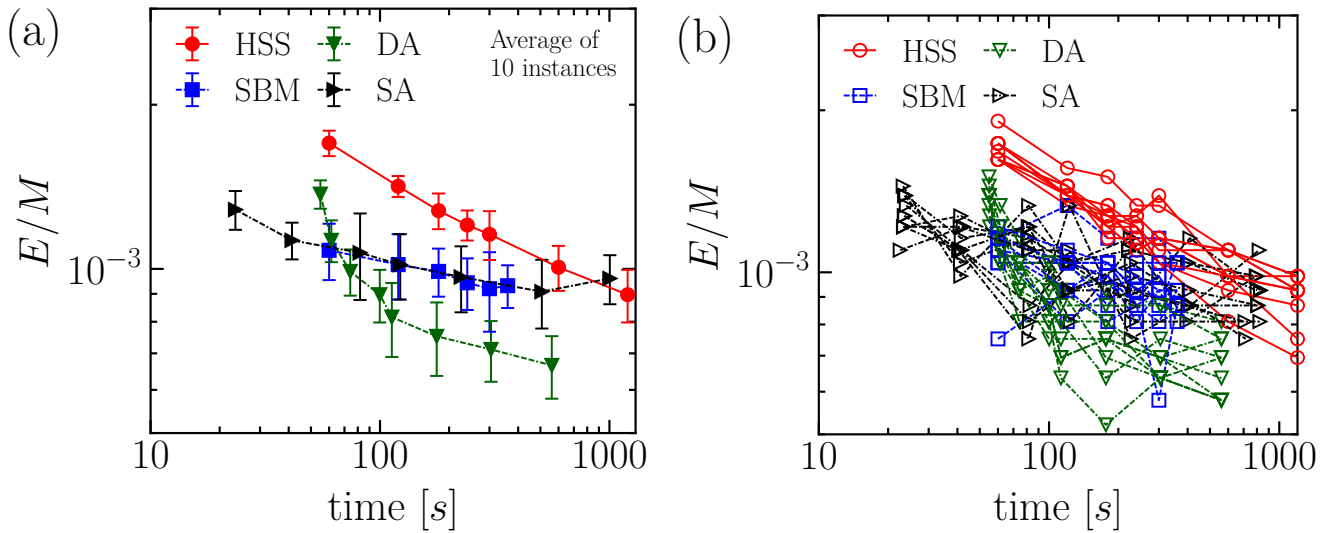


Figure 1. Value of the cost function per clause as a function of the execution time, obtained for NAE 3-SAT with a number of variables $N = 8192$ and a number of clauses $M = 17285$, i.e., $M/N \approx 2.11$. Each data point was obtained from an independent run. See the main text for the time metric of each solver. (a) Average of ten instances. The error bars denote standard deviation. For DA and SA, the execution time was also averaged. (b) Results for ten different instances.

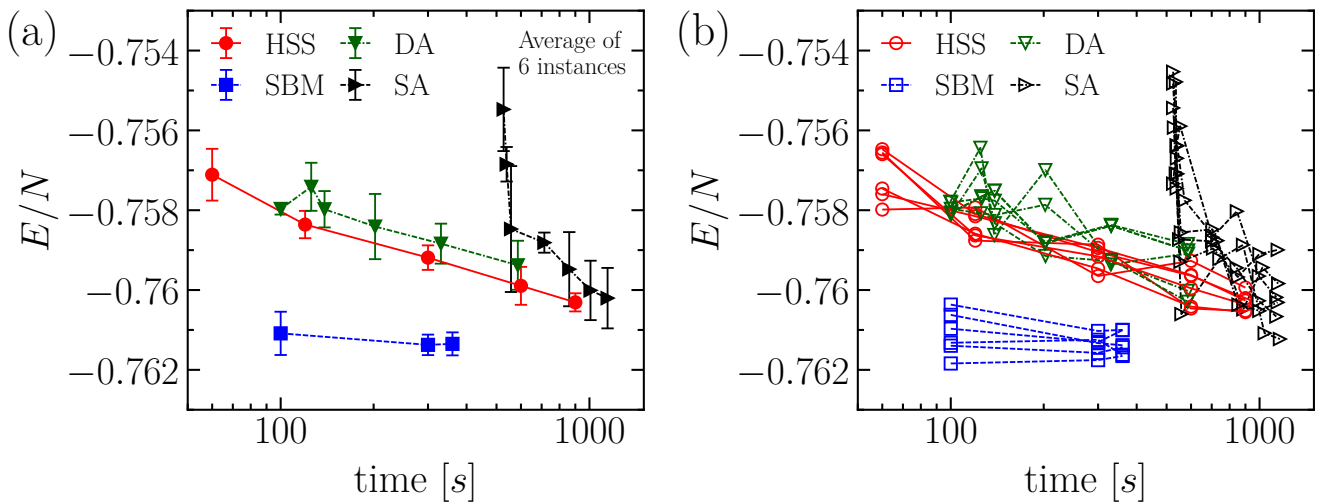


Figure 2. Value of cost function per variable as a function of the execution time, obtained for the SK model with a number of variables $N = 8192$ and $J = 1$. Each data point was obtained from an independent run. See the main text for the time metric of each solver. (a) Average of ten instances. The error bars denote standard deviation. For DA and SA, the execution time was also averaged. (b) Results for six different instances.

input	value of cost function	solvers
g000989	-2322	HSS, SBM, DA
g003215	-821734	HSS
g001269	-45661	HSS, SBM, DA
g000421	-41680.2	HSS, SBM
g002440	-2000460	HSS, SBM, SA
g000432	-188363.1	HSS
g000524	-4335188	HSS, SBM, DA, SA
g002586	-7161694	HSS, SBM
g001327	-9267492	HSS, SBM
g001469	-1.42273e+07	HSS
g002600	-41194.45	HSS
g000969	-6647406	HSS, SBM
g002898	-1.276648e+07	HSS, SBM, DA
g001581	-730413.1	SBM
g000788	-1962898	HSS
g000377	-445529	DA
g002569	-5.084731e+08	HSS
g001086	-3819.935	SA
g001337	-4634430	DA
g000283	-337340.8	SA
g002512	-327679.6	DA
g000802	-2819460	SBM
g003059	-3782885	DA
g002332	-4586683	SA
g002034	-698788.1	HSS
g003198	-1.373565e+08	HSS
g002207	-6781175	HSS, SBM, DA
g001913	-1177002	HSS
g001393	-358732	SBM, DA
g002370	-5.622634e+07	SA
imgseg-216041	-9572357	HSS
imgseg-376020	-1.376284e+07	HSS
g001883	-403013.1	SBM
g000644	-132820	SBM
g000476	-106794	DA
g002312	-2.867864e+07	DA
g002563	-5.848182e+07	DA
g000495	-1.638467e+07	DA
g002204	-1.229112e+08	HSS, SBM, DA
g000503	-8.506962e+07	DA
g002527	-8261389	DA
g001345	-4.011876e+07	SA
p7000-2	-1.824995e+07	DA
g002300	-9.409027e+07	DA
g001651	-130005.8	DA

Table 11. The lowest values of cost function found in this benchmarking for MQLib instances.